Proceedings of the 21st ICSMGE, Vienna, Austria, 14 – 19 June 2026. Pistrol, Adam & Schweiger (eds.)
Published by: ÖGG, Austrian Society for Geomechanics, Salzburg, Austria, ISBN 978-3-9503898-4-5
https://doi.org/10.53243/ICSMGE2026-1720

A unified framework for estimating monotonic and dynamic parameters of sand-silt mixtures through the equivalent intergranular theory

Anthi Papadopoulou
Researcher, Dr. Civil Engineer, Thessaloniki, Greece, anthipapadopoulou4@gmail.com

ABSTRACT: In nature, the granular soil mixtures are predominant and therefore understanding their monotonic and dynamic behavior is an essential tool for geostructures designing. For this purpose, the paper presents results from monotonic triaxial, cyclic triaxial, bender element and resonant column tests to capture the granular soils behavior. Four different granular soil mixtures were formed mixing three clean sands with two non-plastic silts and a gravel with a clean sand, all having different values of the coarse grains mean diameter, D_{50}, to the finer grains mean diameter, d_{50}, ratio. Critical State Lines, CSLs, liquefaction resistance, CRR_{15}, shear wave velocity, V_s, shear modulus, G_{max}, and damping ratio, D_{min}, are the key monotonic and dynamic parameters investigated. In order to account for the contribution of fines content, f_c, to the mixtures structure, the equivalent state concept was used, according to which the mixtures density is adequately represented by the equivalent intergranular void ratio, $(e_g)_{eq}$, for f_c values lower than the threshold, f_{cth}, and by the equivalent interfine void ratio, $(e_f)_{eq}$, for higher f_c, values. Parameters b, and m, introduced in $(e_g)_{eq}$, and $(e_f)_{eq}$, calculation, respectively, recognize that different f_c, contribute differently to the strength of the sand and their values are estimated in order to determine single CSLs, CRR_{15}, V_s, G_{max}, and D_{min}, curves, independently of, f_c, for the tested mixtures based on the results of the laboratory tests. It is shown that parameters b and m, depend on f_c, the loading type of the laboratory test conducted, the shape of grains and on the D_{50}/d_{50}, D_{10}/d_{50}, ratios, while $(e_g)_{eq}$ and $(e_f)_{eq}$, prove to be a suitable parameter for the estimation of monotonic and dynamic behaviour, independently of f_c. The effectiveness of state parameter, ψ, and equivalent state parameters, $(\psi_g)_{eq}$, and $(\psi_f)_{eq}$, in the estimation of the monotonic and dynamic behaviour, is confirmed.

KEYWORDS: critical state, liquefaction, equivalent intergranular void ratio, interfine, shear wave velocity, shear modulus, sand, silt

1 INTRODUCTION

Understanding how the addition of fines affects the monotonic and dynamic behavior of granular soils, in conjunction with the effect of stress and density, constitutes a major challenge in Geotechnical Engineering. The Critical State Lines, CSLs, liquefaction resistance, CRR_{15}, shear wave velocity, V_s, small strain shear modulus, G_{max}, and small strain damping ratio, D_{min}, are key monotonic and dynamic parameters used for soil characterization in common geotechnical engineering practice and constitutive modelling of soil behavior.

In laboratory studies, sands containing fines are considered as consisting of two matrices, the sand grains and the fine grains and their behavior is analyzed in terms of the interaction with each other. There is a threshold fines content, f_{cth}, up to which the mixtures behaviour is governed by the sand skeleton and thereafter by the fines' skeleton, the existence of which has been also observed by other researchers (Thevanayagam, 1998; Polito & Martin 2001). The f_{cth} is an important parameter determining the transition from the sand-dominated to the silt-dominated behaviour of mixtures and is related to their particle packing, mean diameter ratio, and separation distance as well as gradation, mineralogy, and particle shape characteristics (Papadopoulou & Tika 2008). The nature of the contribution of the fines' matrix may be expressed in terms of the intergranular void ratio, e_g, Mitchell (1976):

$$e_g = \frac{e_c + f_c}{1 - f_c} \tag{1}$$

where e_c is the void ratio after consolidation, while for mixtures with, $f_c > f_{cth}$, the interfine void ratio may be more appropriate, according to Thevanayagam & Mohan (2000):

$$e_f = \frac{e_c}{f_c} \tag{2}$$

Thevanayagam (2000) introduced an additional parameter, b ($0<b<1$), in e_g, expression to account for the fines which actually contribute to the maintenance of the grains contacts, proposing for $f_c \le f_{cth}$, the $(e_g)_{eq}$:

$$(e_g)_{eq} = \frac{e_c + (1-b)\cdot f_c}{1 - (1-b)\cdot f_c} \tag{3}$$

Parameter b recognizes that different f_c values contribute differently to sand's strength. A value of b=1 indicates that the total of fines, actively participate in sustaining the imposed forces, while in the absence of fines, $f_c=0$, the $(e_g)_{eq}=e_c$.

For $f_c > f_{cth}$, the equivalent interfine void ratio $(e_f)_{eq}$, may be considered as active contacts index, Thevanayagam (2000):

$$(e_f)_{eq} = \frac{e_c}{f_c + \frac{(1-f_c)}{R_d^m}} \tag{4}$$

where m ($0<m<1$), is a coefficient that depends on grains characteristics and packing and $R_d=D_{50}/d_{50}$ is the ratio of the coarse to the fine grains mean diameters.

According to the CS concept, the behavior of a sand depends not only on density, but also on stress. A sand's true state is described by the location of its current stress and volume state relative to the CSL. This distance has been quantified by means of a state parameter, $\psi=e-e_{cs}$, (Been & Jefferies 1985), which is the difference in void ratios between the current state and the CSL at the current p'_{cs}. The equivalent state parameters, $(\psi_g)_{eq}$, $(\psi_f)_{eq}$, correspond to $(e_g)_{eq}$, and $(e_f)_{eq}$, respectively.

In this study we assess the monotonic and dynamic behaviour of four different granular soil mixtures, formed by mixing three clean sands with two non-plastic silts and a gravel with a clean sand, all having different values of the R_d, ratio. The objective is to estimate the values of b and/or m, and consequently $(e_g)_{eq}$ and/or $(e_f)_{eq}$ to determine single CSLs, CRR_{15}, V_s, G_{max}, and D_{min}, curves, independently of f_c. The effects of f_c, loading type of the laboratory test conducted, shape and size of grains through R_d, and disparity ratio, $x=D_{10}/d_{50}$, on b, and m, are investigated together with $(e_g)_{eq}$, $(e_f)_{eq}$, suitability to estimate the mixtures monotonic and dynamic behaviour, independently of f_c The effectiveness of ψ, $(\psi_g)_{eq}$, and $(\psi_f)_{eq}$, in monotonic and dynamic behaviour estimation, is also investigated.

2 TESTING PROGRAMME

2.1 *Tested materials*

The materials used in the testing program were three natural clean sands, S1, S2, S3, two non-plastic silts, F1, F2 and a gravel G1. The physical properties and the grain size distributions of the tested materials are presented in Table 1, and Figure 1, respectively.

Table 1. Physical properties of the tested materials.

Soil	G_s	D_{50} (mm)	C_u	e_{min}	e_{max}	Grains shape
S1	2.649	0.30	1.3	0.582	0.841	Well Rounded
S2	2.665	0.76	1.7	0.673	0.967	Sub Angular
S3	2.746	0.19	1.8	0.767	1.082	Sub Angular
F1	2.663	0.02	7.5	0.658	1.663	Angular
F2	2.718	0.04	8.7	-	-	Angular
G1	2.681	2.35	3.9	0.576	0.787	Rounded

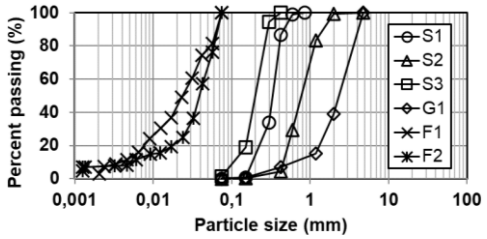

Figure 1. Grain size distributions of the tested materials.

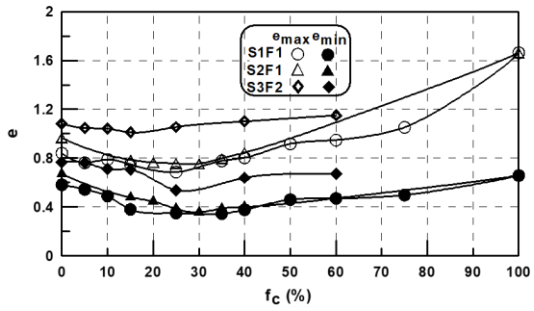

Figure 2. Variation of index void ratios, e_{min} and e_{max}, of the tested materials with f_c.

Monotonic triaxial, TX, tests, were conducted on mixtures of S1 with F1, S2 with F1, and G1 with S2, at the by weight percentages of 0, 5, 10, 15, 25, 35, 40, 60 and 100%, at 0, 15, 20, 25, 30, 35, 40 and 100%, and at 30, 40, 50, 60 and 100%, respectively. Resonant column, RC, tests were conducted on mixtures of S3 with F2, at 0, 5, 10, 15, 25, 40 and 60%. Cyclic triaxial, CTX, tests were conducted on mixtures of S1 with F1, at 0, 5, 15, 25, 35, 40, 60 and 100% while at the percentages of 0, 15, 25 and 35%, bender element, BE, tests were conducted prior to cyclic loading.

For the determination of the minimum void ratio, e_{min}, both the vibratory table and the standard proctor test methods were used. The maximum void ratio, e_{max}, was determined by pouring in a mould dry material three times repeatedly and considering the average as the e_{max} value. Figure 2, presents the e_{min} and e_{max}, variations with f_c, for S1F1, S2F1 and S3F2.

2.2 *Testing equipment and experimental procedures*

The testing programme consisted of monotonic, bender element and cyclic triaxial tests for the determination of CSLs, V_s and CRR_{15}, of the tested materials, respectively. The tests were performed using a closed-loop automatic cyclic triaxial apparatus (MTS Syst. Corp., U.S.A.). For the determination of G_{max}, and D_{min}, a resonant-column apparatus of the fixed-free type was used (Drnevich, 1967). A detailed description of apparatuses' principles of operation and testing procedures is given in Papadopoulou (2008) and Papadopoulou (2002).

When using the CTX apparatus, the specimens (height/diameter≈100/50mm) were formed by moist tamping at a varying water content, 4-12% for all tested materials and 35% only for the silt specimens, using the undercompaction method, (Ladd, 1978). Moist tamping was preferred to other preparation methods, as it produces specimens of varying densities (Verdugo & Ishihara 1996). Saturation was achieved by percolating through the specimen CO_2 from the bottom to the top drainage line and then de-aired water. A suction pressure of 15kPa was applied while dismantling the specimen, measuring its dimensions, and assembling the triaxial cell. In order to ensure full saturation, a series of steps of simultaneous increasing cell pressure and back pressure were performed, while maintaining an effective confining stress of 15 kPa. Parameter B had values 0.95-1.0. After the completion of saturation, the specimens were isotopically consolidated under an effective isotropic stress, p'_0, ranging from 50 to 625kPa. A period of time equal to double the consolidation time of the specimens was allowed before shearing. During consolidation the volume change and the axial displacement of the specimens were recorded in order to calculate the post consolidation void ratio. In TX tests, specimens were subjected to undrained compression at an axial displacement of 0.05mm/min. In CTX tests, a sinusoidally varying axial stress ($\pm\sigma_d$) was applied at 0.1Hz frequency under undrained conditions. The cyclic stress ratio, $CSR=\sigma_d/2p'_0$, corresponds to double amplitude axial strain, $\varepsilon_{DA}\approx5\%$ and liquefaction resistance, CRR_{15}, is defined as the CSR required to cause $\varepsilon_{DA}\approx5\%$ at 15 cycles of loading.

The bender element system was installed in the CTX apparatus. An Agilent 33220 function generator for the excitation of the top platen source sensor with an electrical signal and an Agilent 54642A digital oscilloscope for displaying and recording the input-source and output-receiver signals, were connected to a computer. A sinusoidal pulse of 10 Volts amplitude at a 3-10kHz frequency was used. For shear wave travel time measurement in soil specimen the start-to-start method was used (Kawaguchi et al. 2001). To account for the near field effect disturbances and signal noises, signal arrival was observed by passing waves of different frequencies (Brignoli et al. 1996; Lee & Santamarina 2005). As the BE test is considered non-destructive, measurements of V_s were performed at various levels of p'_0=30-300kPa. A detailed description of the BE and the automated measurements system developed for signal acquisition and analyses is given in Theopoulos et al. (2009) and Papadopoulou & Tika (2021).

In the resonant-column apparatus, for G_{max}, determination defined as the initial shear modulus measured in the small shear strain range, which is almost constant, and D_{min}, solid cylindrical specimen, having platens attached to each end, and nominal dimensions height/diameter≈142mm/71mm, were prepared using undercompaction (Ladd, 1978). After saturation, consolidation was performed at the isotropic confining effective stress, σ'_0, 50, 100 and 200kPa. An electromagnetic sinusoidal torsional excitation was imposed to the top platen (free-end). The bottom platen was rigidly fixed (fixed-end). The excitation frequency was adjusted until the specimen's first mode resonance was established. Measurements of resonant frequency, acceleration and amplitude of the applied vibration excitation were made at the free end. The measurements during torsional excitation were then combined with the apparatus characteristics to calculate the specimens shear modulus, G, and damping ratio, D.

3 TEST RESULTS AND ANALYSIS

3.1 *Critical state lines*

The tested mixtures S1F1, S2F1, G1S2 and S3F2, CSLs, are presented in Figure 3, Figure 4, Figure 5, and Figure 6, respectively, in the e-p′$_{cs}$, and $(e_g)_{eq}$ and/or $(e_f)_{eq}$-p'$_{cs}$, planes. For S1F1, S2F1, the CSLs move downwards with increasing f_c up to 35% and then upwards with further increasing f_c, while the CSLs of the mixtures with f_c=35% and 40%, practically coincide. Consequently, for both types of mixtures the f_{cth}, based on the CSLs, is in the range of 35-40%. In the case of G1S2 the CSLs move downwards with increasing f_c up to 50% and upwards with further increasing f_c, while the CSLs of the mixtures with f_c=40% and 50%, practically coincide, showing that the f_{cth}, is in the range of 40-50%. For S3F2, the test data from Billis & Hatzitheodorou (2003) were used to form the CSLs in the e-p′$_{cs}$, plane, and although the data are limited to the f_c of 15%, they are useful in the correlations of G_{max}, and D_{min}, from the RC tests to the state parameters, ψ and $(\psi_g)_{eq}$.

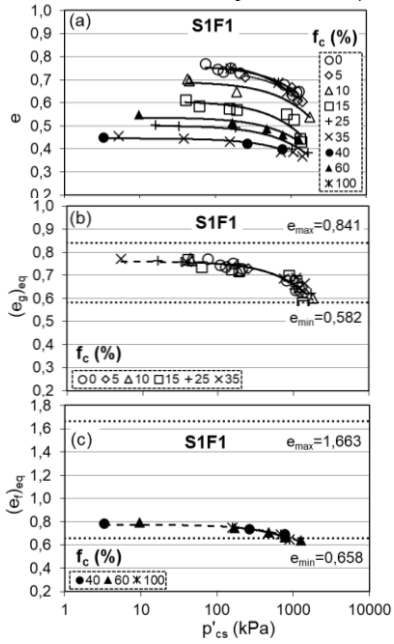

Figure 3. CSLs of S1F1, (a) e-p′$_{cs}$, (b) $(e_g)_{eq}$-p′$_{cs}$, and (c) $(e_f)_{eq}$-p′$_{cs}$.

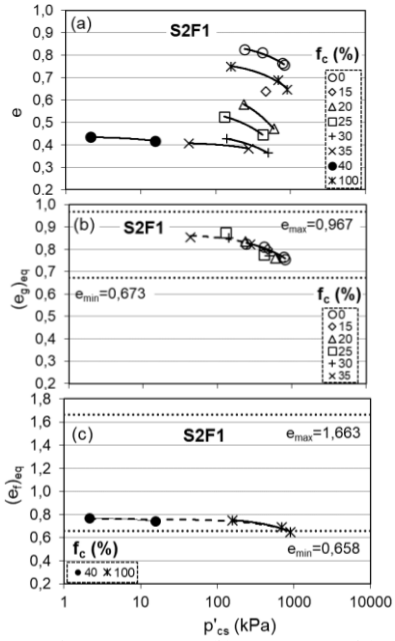

Figure 4. CSLs of S2F1, (a) e-p′$_{cs}$, (b) $(e_g)_{eq}$-p′$_{cs}$, and (c) $(e_f)_{eq}$-p′$_{cs}$.

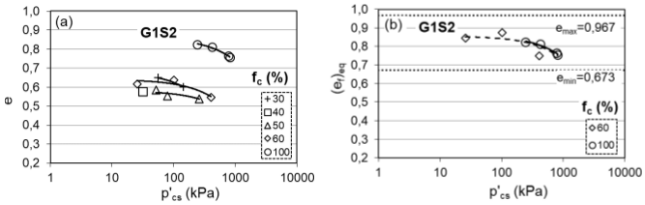

Figure 5. CSLs of G1S2, (a) e-p′$_{cs}$, and (b) $(e_f)_{eq}$-p′$_{cs}$.

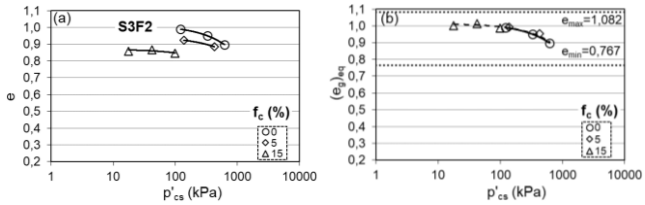

Figure 6. CSLs of S3F2, (a) e-p′$_{cs}$, (Billis & Hatzitheodorou, 2003) and (b) $(e_g)_{eq}$-p′$_{cs}$.

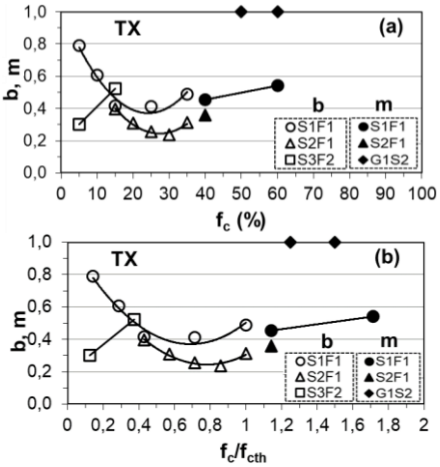

Figure 7. Variation of b and m, with (a) f_c (%) and (b) f_c/f_{cth}.

Parameters b, and m, were calculated based on the criterion of the maximum possible coincidence of each mixture's CSL to that of sand, for $f_c \le f_{cth}$, and to that of silt, for $f_c > f_{cth}$, respectively. For each f_c, a different b, and/or m, value was determined allowing $(e_g)_{eq}$ and/or $(e_f)_{eq}$, calculations. The variations of b, and/or m, with f_c, and f_c/f_{cth}, are presented in Figure 7. For S1F1, S2F1 mixtures, the b variation may be expressed satisfactorily by a quadratic polynomial equation, with its minimum corresponding to an f_c of 25%, lower than the f_{cth}=35%, while for S3F2 mixtures more data are required. For G1S2 mixtures, the sand grains play the role of fines and only the values of m for $f_c > f_{cth}$, were calculated because the gravel's CSL is not available. Using a constant value of b, for all the mixtures cannot represent the b value corresponding to each one of them. The variation of, m, follows the parameter b pattern, although more data are required to conclude that.

3.2 *Liquefaction resistance*

According to the CRR_{15}-e curves for S1F1, given in detail in Papadopoulou (2008), at a given p′$_0$ and e, CRR_{15} decreases with increasing f_c up to f_{cth}, and increases thereafter with further increasing f_c. For S1F1, f_{cth} is 35% and 25% at p′$_0$=50–200kPa and 300kPa, respectively. Moreover, it is shown that at a given density, CRR_{15} decreases with increasing p′$_0$ and that the effect of p′$_0$ on CRR_{15} diminishes with increasing f_c. Figure 8 shows the variations of CRR_{15} with $(e_g)_{eq}$ and/or $(e_f)_{eq}$, ψ, and $(\psi_g)_{eq}$ and/or $(\psi_f)_{eq}$, at p′$_0$=50-300kPa, for S1F1. Parameters b and m were calculated based on the criterion of the maximum coincidence of the CRR_{15} curve of each mixture with $f_c \le f_{cth}$ to that of the sand and each mixture with $f_c > f_{cth}$ to that of the silt. For each p'$_0$, the solid curves represent the

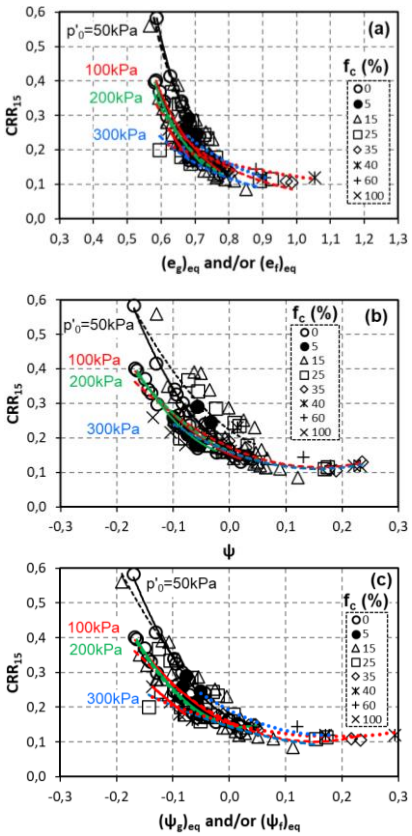

Figure 8. Liquefaction resistance curves of S1F1 on (a) CRR_{15}-$(e_g)_{eq}$, and/or $(e_f)_{eq}$, (b) CRR_{15}-ψ, and (c) CRR_{15}-$(\psi_g)_{eq}$, and/or $(\psi_f)_{eq}$, at p'_0=50, 100, 200 and 300kPa.

sand, the dashed ones the sand and the mixtures with $f_c \leq f_{cth}$, while the dotted ones the silt and the mixtures with $f_c > f_{cth}$, to show their coincidence. There is a decrease of CRR_{15}, with increasing $(e_g)_{eq}$ and/or $(e_f)_{eq}$, ψ, and $(\psi_g)_{eq}$ and/or $(\psi_f)_{eq}$, due to increased contractiveness and also the curves for the stresses 100-300kPa, exhibit great conscience. It is shown that $(e_g)_{eq}$ and/or $(e_f)_{eq}$, may be an appropriate density parameter and together with ψ, can serve as a suitable parameter for the estimation of the monotonic behaviour in relation to the liquefaction resistance in mixtures with fines, irrespectively of their f_c, for the values of p'_0=100, 200 and 300kPa, while the $(\psi_g)_{eq}$ and/or $(\psi_f)_{eq}$, provide even much better correlations. These correlations are very useful as they connect the monotonic behaviour, contractive (ψ>0) or dilative (ψ<0), with the liquefaction resistance for soils such as the tested sands with non-plastic fines, which are commonly encountered in geotechnical engineering works.

3.3 *Shear wave velocity*

The V_s-e curves at various levels of p'_0, for S1F1, are given in detail in Papadopoulou & Tika (2021). An increase of V_s with increasing p'_0, is evident and this increase is significantly greater at the transition of p'_0, from 100 to 200kPa. Moreover, for a given p'_0, V_s increases with decreasing e, as shear waves travel faster in denser specimens. In Figure 9, the V_s-$(e_g)_{eq}$, variations and the V_s normalized to the stress, $V_s/(p'_0)^{n/2}$, variations with ψ, and $(\psi_g)_{eq}$, are presented. Parameter n varies with f_c, (Papadopoulou & Tika 2021). It can be seen that $(e_g)_{eq}$, is a suitable density parameter for estimating the mixtures' V_s. The V_s-ψ, correlation is not useful for the estimation of the monotonic behaviour in relation to the V_s, due to the fact that the V_s, of the tested mixtures was significantly lower than that of the sand something that $(\psi_g)_{eq}$,

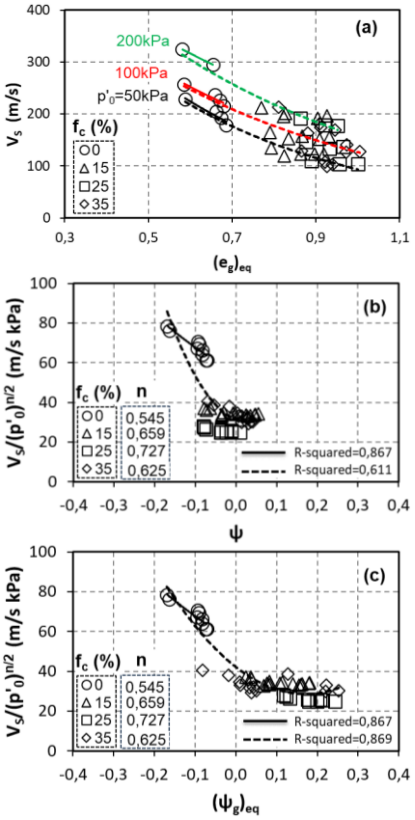

Figure 9. Shear wave velocity curves of S1F1 on (a) V_s-$(e_g)_{eq}$, at p'_0=50, 100, and 300kPa, (b) $V_s/(p'_0)^{n/2}$-ψ, and (c) $V_s/(p'_0)^{n/2}$-$(\psi_g)_{eq}$.

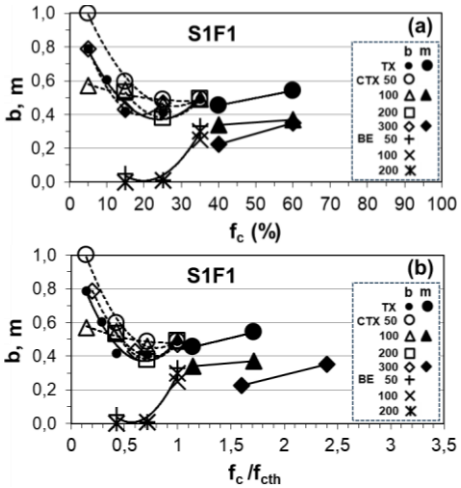

Figure 10. Variation of b and m, from monotonic, cyclic triaxial and bender element tests, for S1F1, with (a) f_c (%) and (b) f_c/f_{cth}.

could capture, since it takes into account only the fines that contribute to sustaining the imposed to soil skeleton stresses.

Figure 10, shows the b, m, variations with f_c, and f_c/f_{cth}, as estimated from TX, CTX and BE tests, for S1F1, at various p'_0, values. Parameter b estimated from CTX tests depends on f_c and p'_0, and its variation with f_c may be expressed satisfactorily by a quadratic polynomial equation, while its minimum values correspond to an f_c of 25% lower than the threshold, f_{cth}=35% in the cases of p'_0=50, 100 and 200kPa, and an f_c of 15% lower than the threshold, f_{cth}=25% in the case of p'_0=300kPa. With increasing p'_0, the values of b tend to decrease. It is worth noting that the b-f_c and b-f_c/f_{cth} curves, as derived from the TX tests results, form a lower band since the b values estimated from the CTX tests results are higher with the exception of the mixture of the sand with 5% fines at the

p'_0=100kPa. The variations of parameter m, from CTX tests, calculated at p'_0=100 and 300kPa, seem to follow the b variation pattern but their values are at a lower level. For parameter b, as calculated from BE tests, a completely different trend is evidenced, with its values being practically at zero level, for the values of f_c up to 25% and increasing thereafter up to the f_{cth}=35%, and they don't depend on stress. This depicts the very low V_s values of the tested mixtures. It can be concluded that parameters b and m, besides f_c depend also on the loading type of the laboratory test conducted.

3.4 *Small strain shear modulus and damping ratio*

In Figure 11 and Figure 12, the maximum shear modulus and damping ratio curves with e, $(e_g)_{eq}$, ψ, and $(\psi_g)_{eq}$, are presented for S3F2 at σ'_0=42-217kPa. The G_{max}-e curves move downwards with increasing f_c up to 40% and increase thereafter with further increasing f_c, showing that the f_{cth}=40%. Due to the fact that tests on pure silt were not conducted, the calculation of m, was not possible. The D_{min}-e curves move downwards with increasing f_c up to 60%, and so no f_{cth} was identified, while D_{min} is not affected by stress level. Again, $(e_g)_{eq}$, may be efficient as a density parameter while ψ, and $(\psi_g)_{eq}$, practically they are equally sufficient in connecting the monotonic and dynamic behaviour of the materials tested. In Figure 13, it is shown that the b-f_c variations from RC tests, follow a different trend. Values of b based on G_{max} decrease with increasing f_c up to 15% and increase thereafter up to the f_{cth}, while the effect of σ'_0, also diminishes for $f_c \geq 15\%$. As far as D_{min} is concerned, b increases with increasing f_c up to 40% and stabilizes thereafter, where the σ'_0, effect also diminishes.

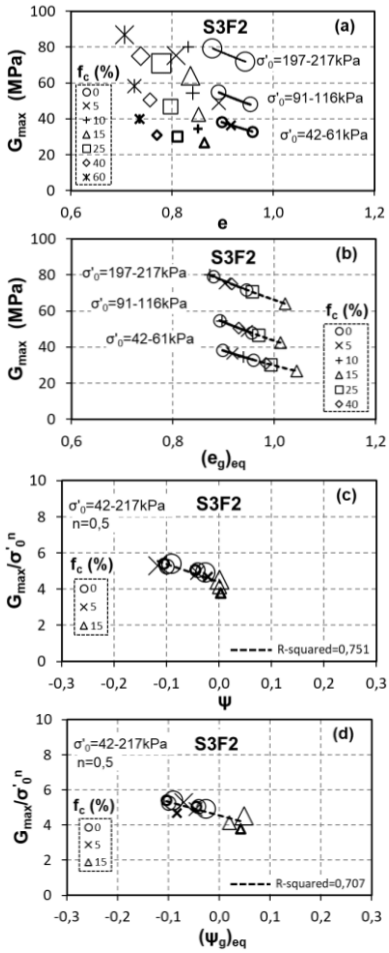

Figure 11. Shear modulus curves of S3F2 on (a) G_{max}-e, and (b) G_{max}-$(e_g)_{eq}$, at σ'_0=42-217kPa, (c) $G_{max}/(\sigma'_0)^n$-ψ, and (c) $G_{max}/(\sigma'_0)^n$-$(\psi_g)_{eq}$.

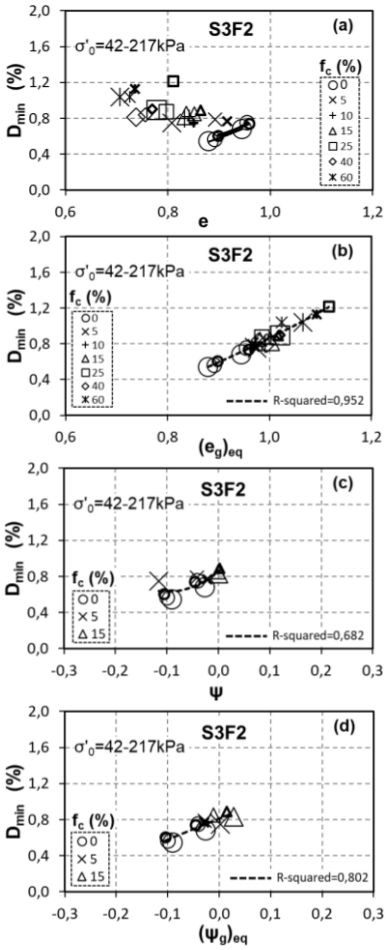

Figure 12. Damping ratio curves of S3F2 on (a) D_{min}-e, (b) D_{min}-$(e_g)_{eq}$, (c) D_{min}-ψ, and (c) D_{min}-$(\psi_g)_{eq}$, at σ'_0=42-217kPa.

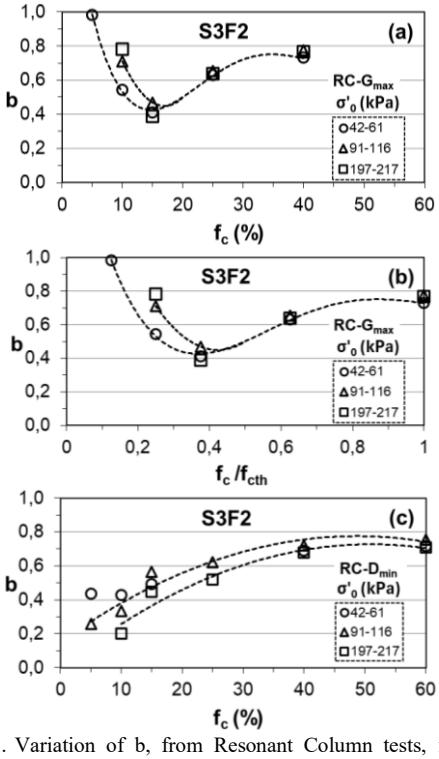

Figure 13. Variation of b, from Resonant Column tests, for S3F2, from G_{max} with (a) f_c, (%) and (b) f_c/f_{cth}, and from D_{min} with (c) f_c (%).

4 EFFECTS OF GRAINS CHARACTERISTICS

We attempt to capture the influence of the size and shape of mixtures grains in the b, m, values. In Figure 14, we compare the b, m, values from TX tests, of mixtures with different shapes of grains and different x and R_d values. We consider that each mixture's characterization, regarding the shape of its grains, changes with increasing f_c. For example, S1F1 with f_c=5% may be characterized as Well Rounded since the sand grains prevail, but when f_c=35% the mixture is characterized as Sub Rounded-Sub Angular due to the increased percent of the Angular shaped silt grains. As the content of the angular in shape fines increases, angularity increases. For a given x value, parameter b receives lower values as angularity increases with the variations being more evident when f_c is low, and they tend to coincide when f_c approaches the f_{cth}. As x increases the b, m, values decrease and tend to coincide for 15<x<25 around a range of values from 0.2-0.4. These findings are also consistent for the b-R_d relations which also tend to coincide for 30<R_d<40 around a range of values from 0.2-0.4.

The b, m, values from the dynamic tests, CTX, BE, RC, should be compared to corresponding values from the results of other researchers to proceed to conclusions.

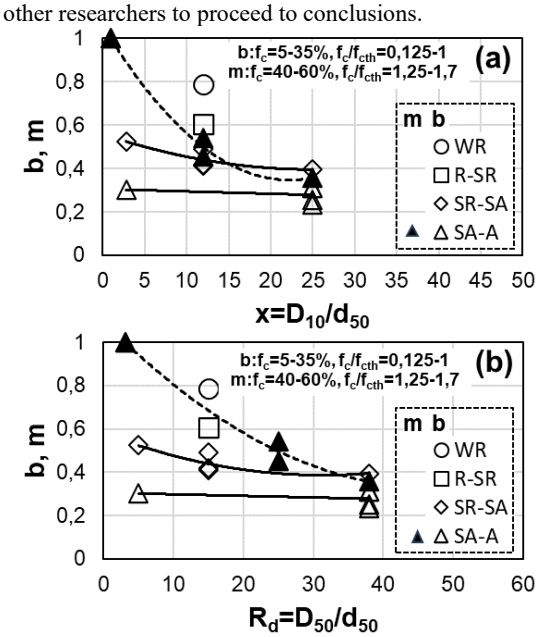

Figure 14. Variation of b and m, from TX tests in relation to the mixtures' grains shape with (a) x and (b) R_d.

5 CONCLUSIONS

From the results of the present study the following conclusions can be drawn:

Parameters b, and m, depend on the fines content, f_c, and on the loading type of the laboratory test conducted. The b-f_c and m-f_c curves present different patterns in regard to the type of test conducted and the materials' properties measured.

The shape of the mixtures' grains (Angular, Sub-Angular, Sub-Rounded, Rounded, or Well-Rounded) has a significant role in the estimation of parameter b of granular mixtures and should be considered in combination with parameters R_d=D_{50}/d_{50} and x=D_{10}/d_{50}, as well as the f_c and the f_{cth}.

The equivalent intergranular, $(e_g)_{eq}$, and interfine $(e_f)_{eq}$, void ratios, are appropriate density parameters for the expression of the monotonic and dynamic behavior of granular mixtures, through unique CSLs, CRR_{15}, V_s, G_{max}, and D_{min}, curves, irrespective of f_c.

The equivalent state parameters, $(\psi_g)_{eq}$, $(\psi_f)_{eq}$, can be sufficiently used for the estimation of the monotonic and dynamic behaviour of granular mixtures, since they capture the content of fines that actually participate in sustaining the streeses imposed to the soil skeleton. The state parameter, ψ, is also useful, but failed to estimate the mixtures behaviour in the case of the BE tests. These correlations should be used with engineering judgement in the cases of contractive behaviour, (ψ>0, $(\psi_g)_{eq}$,>0, $(\psi_f)_{eq}$,>0).

The equivalent concept proves to be a useful tool and may capture the degree of the fines' participation in the monotonic and dynamic behaviour of granular mixtures, for practical purposes.

The proposed relations, likely enriched with more data, may be used as a tool for an accurate estimation of parameters b, m, with respect to f_c, f_{cth}, angularity or roundness of the grains shape and x, or R_d, values, for sand-silt mixtures.

6 REFERENCES

Been, K., and Jefferies, M.G., 1985. A state parameter for sands. *Géotechnique*,35(2), 99-112.

Billis, T., and Hatzitheodorou, N., 2003. Study of soil liquefaction and its countermeasures. *Diploma Thesis*. Aristotle University of Thessaloniki, Greece (in Greek).

Brignoli, E.G.M., Gotti, M., and Stokoe, K.H. II., 1996. Measurement of shear waves in laboratory specimens by means of piezoelectric transducers. *Geotechnical Testing Journal*, 19, 384–397.

Drnevich, D., 1967. Effects of strain history on the dynamic properties of sand. *PhD. Thesis*, University of Michigan.

Kawaguchi, T., Mitachi, T., and Shibuya, S., 2001. Evaluation of shear wave travel time in laboratory bender element test. *Proc. 15th International Conference on Soil Mechanics and Geotechnical Engineering*, Istanbul, 155-158.

Ladd, R.S., 1978. Preparing test specimens using undercompaction. *Geotechnical Testing Joural*, 1(1), 16–23.

Lee, J.S., and Santamarina, J.C., 2005. Bender Elements: Performance and Signal Interpretation. *Journal of Geotechnical and Geoenvironmental Engineering ASCE*, 131, 1063–1070.

Mitchell, J.K. 1976. *Fundamentals of soil behavior*. New York: John Wiley and Sons Incorporated.

Papadopoulou, A., and Tika, Th., 2021. Laboratory - based correlation between liquefaction resistance and shear wave velocity of sand with fines. *Geotechnics*, 1(2), 219-242.

Papadopoulou, A., and Tika, T., 2008. The effect of fines on critical state and liquefaction resistance characteristics of non-plastic silty sands. *Soils and Foundations*, 48(5), 713–725.

Papadopoulou, A.I., 2008. Laboratory investigation into the behavior of silty sands under monotonic and cyclic loading. *PhD Thesis*, Aristotle University of Thessaloniki, Greece (in Greek).

Papadopoulou, A., 2002. The effect of fines content on the liquefaction resitance of sandy soils. *Dissertation Thesis*, Aristotle University of Thessaloniki, Greece (in Greek).

Polito, C.P., and Martin, II. J.R., 2001. Effects of nonplastic fines on the liquefaction resistance of sands. *Journal of Geotechnical and Geoenvironmental Engineering*, 127(5), 408-415.

Theopoulos, A.; Papadopoulou, A.; Tika, Th. and Laopoulos Th... An automated system for measurement of shear waves velocity in soil. In Proceedings of the XIX IMEKO World Congress Fundamental Applied Metrology, Lisbon, Portugal, 6–11 September 2009; pp. 1597–1600. 32.

Thevanayagam, S., 2000. Liquefaction potential and undrained fragility of silty sands. *Proc. 12th International Conference on Earthquake Engineering*, Auckland, 2383.

Thevanayagam, S., and Mohan, S., 2000. Intergranular state variables and stress-strain behaviour of silty sands. *Géotechnique*, 50(1), 1-23.

Thevanayagam, S., 1998. Effect of fines and confining stress on steady state strength of silty sands. *Journal of Geotechnical Engineering, ASCE*, 124, 479–491.

Verdugo. R., and Ishihara, K., 1996. The steady state of sandy soils. *Soils and Foundations*, 36(2), 81–91.